

SPATIOTEMPORAL SUB PIXEL MAPPING OF TIME-SERIES IMAGES

Raghava M S,

Assistant Professor, Department of Computer science engineering,
Sambhram institute of technology, Bangalore, Karnataka

ABSTRACT

LCLU monitoring is a trending topic of research now. Sub pixel mapping (SPM) can be used to extract the LCLU information of by dividing the pixels into sub pixels. Application of SPM technique for Time series images (TSIs) is a very rare condition or topic of research. This paper includes research work conducted on TSIs using the SPM technique for LCLU monitoring. In this work both the spatial and temporal dependencies are considered simultaneously. The spatial dependencies are considered by correlation of the sub pixels within each image whereas the temporal dependencies consider a correlation of sub pixel classes between images. The main aim of the proposed method is to maximize the spatiotemporal dependence, which is defined by blending both spatial and temporal dependences. Experiments on conducted showed that the proposed approach can provide more accurate sub pixel resolution of the TSIs than the existing SPM methods. The SPM results obtained from the TSIs provide an excellent opportunity for LCLU dynamic monitoring and change detection at a finer spatial resolution than the available coarse spatial resolution TSIs.

Keywords: LCLU monitoring, Sub pixel mapping (SPM), Time series images (TSIs)

INTRODUCTION

LCLU monitoring is a delineable area of the earth's terrestrial surface, including all attributes of the biosphere immediately above or below the surface. Which includes surface climate, soil and terrain forms, surface hydrology including shallow lakes, rivers, marshes and swamps, surface sedimentary layers and associated groundwater and geo hydrological reserves, plant and animal populations, human settlement pattern and physical results of past and present human activity (terracing, water storage or drainage structures, roads, buildings, etc.)

Land cover (LC) is a Physical and biological cover of the earth's surface including artificial surfaces, agricultural areas, forests, natural areas, wetlands, water bodies. Land use (LU) is a Territory characterized according to its current and future planned functional dimension or socio-economic purpose (e.g. residential, industrial, commercial, agricultural, forestry, recreational).

Functional definition of LU describes the land in terms of its socio-economic purpose (e.g. agricultural, residential, forestry). In this LU can be inferred from LC

Sequential definition of LU describes the land based on series of operations on land, carried out by humans, with the intention to obtain products and/or benefits through using land resources. Here LU cannot be inferred from LC. Other information sources are needed.

The Users of LCLU information are the Agencies responsible for policy implementation and enforcement, Information providers, Industries and businesses that are often the target of policy, NGOs and the public, Research bodies, Policy makers (e.g. DG from EC, EEA, National, Member States Agencies).

The main sources of the images for LCLU monitoring are Landsat and MODIS sensors as they are freely available, regularly revisits the capabilities, and due to their wider swath.

SUB PIXEL MAPPING OR SUPER RESOLUTION MAPPING (SPM)

SPM, which is also termed super resolution mapping in remote sensing, is a technique that can be achieved through the post processing of spectral unmixing. In SPM each pixel is divided into number of subpixels. The number of sub pixels in each class is determined by spectral unmixing output and by using the zoom factor. SPM assumes that the land cover is spatially dependent both within and between pixels (i.e., compared with more distant pixels, neighboring pixels are more likely to be of the same class). Based on this assumption subpixel classes are predicted. SPM transforms pixel-level unmixing outputs (i.e., coarse LCLU proportions) into a finer spatial resolution hard classification, and this allows a hard classification technique to be applied at the sub pixel level.

The advantages of SPM are as follows.

- In SPM both spatial and temporal dependencies are fused together. Therefore the information capitulation occurs more deeply in TSIs.
- Accuracy is more in SPMs
- Weights are calculated without any human intervention. Thus it is completely automatic.
- The approach offers an excellent opportunity for LCLU dynamic monitoring and change detection at a finer spatial resolution than the available coarse TSIs

The remaining sections of the paper involves the related work, proposed method, Experimental result conclusion and the references.

RELATED WORK

Many experiments and research works have been carried out from last few decades on LCLU monitoring of the TSIs. Few methods available for LCLU monitoring of the TSIs are Bayesian classification [1], compound classification [2-3], spatiotemporal Markov random

fields[4-6], domain adaption[7] , and spatiotemporal segmentation [8]. these techniques are based on pixel-level LCLU classification of all the images in the time series and explicit use of the temporal correlation between images in the form of, for example, transition probabilities or joint probabilities between LCLU classes.

The existing SPM algorithms are genetic algorithms[9], particle swarm optimization [10], pixel swapping algorithm (PSA)[11-12], Hopfield neural network [13-14], maximum *a posteriori* method[15], subpixel/pixel spatial attraction model (SPSAM)[16-17], backpropagation neural network[18-19], Kriging [20], indicatorCokriging [21-22], Markov random field[23-24], contouring method[25] , and the newly developed soft-thenhard SPM framework. In all of these algorithms, spatial dependence is described in different ways. Traditional hard classification approaches cannot be applied because of sub-pixel heterogeneity.

In this paper, a new spatiotemporal SPM algorithm is proposed for multi temporal LCLU mapping from coarse TSIs. The spatiotemporal dependence at the sub pixel scale is defined by fusing the spatial dependence with the temporal dependence.

For large areas, it is difficult to assess the spatial distribution and inter-annual variation of crop acreages through field surveys. Time series of coarse resolution imagery offer the advantage of global coverage at low costs, and are therefore suitable for large-scale crop type mapping. Due to their coarse spatial resolution, however, the problem of mixed pixels has to be addressed. In this work author evaluate neural networks as a modeling tool for sub-pixel crop acreage estimation. The proposed methodology is based on the assumption that different cover type proportions within coarse pixels prompt changes in time profiles of remotely sensed vegetation indices like the Normalized Difference Vegetation Index (NDVI). Neural networks can learn the relation between temporal NDVI signatures and the sought crop acreage information. This learning step permits a non-linear unmixing of the temporal information provided by coarse resolution satellite sensors. For assessing the feasibility and accuracy of the approach, a study region in central Italy (Tuscany) was selected [1].

Due to rapid changes on the Earth's surface, it is important to perform land cover change detection (CD) at a fine spatial and fine temporal resolution. However, remote sensing images with both fine spatial and temporal resolutions are commonly not available or, where available, may be expensive to obtain. This paper attempts to achieve fine spatial and temporal resolution land cover CD with a new computer technology based on sub pixel mapping (SPM): The fine spatial resolution land cover maps (FRMs) are first predicted through SPM of the coarse spatial but fine temporal resolution images, and then, subpixel resolution CD is performed by comparison of class labels in the SPM results. For the first time, five fast SPM algorithms, including bilinear interpolation, bicubic interpolation, subpixel/pixel spatial attraction model,

Kriging, and radial basis function interpolation methods, are proposed for subpixel resolution CD. The auxiliary information from the known FRM on one date is incorporated in SPM of coarse images on other dates to increase the CD accuracy. Based on the five fast SPM algorithms and the availability of the FRM, subpixels for each class are predicted by comparison of the estimated soft class values at the target fine spatial resolution and borrowing information from the FRM. Experiments demonstrate the feasibility of the five SPM algorithms using FRM in subpixel resolution CD. They are fast methods to achieve subpixel resolution CD [2].

Slow-moving landslides are widespread in many landscapes with significant impacts on the topographic relief, sediment transfer and human settlements. Their area-wide mapping and monitoring in mountainous terrain, however, is still challenging. The growing archives of optical remote sensing images offer great potential for the operational detection and monitoring of surface motion in such areas. This study proposes a multiple pair wise image correlation (MPIC) technique to obtain a series of redundant horizontal displacement fields, and different multi-temporal indicators for a more accurate detection and quantification of surface displacement. The technique is developed and tested on a series of monoscopic and stereoscopic Pléiades satellite images at a test site in the South French Alps. Empirical tests confirm that MPIC significantly increased detection accuracy (F-measure = 0.85) and that the measurement error can be reduced by averaging velocities from all pair combinations covering a given time-step (i.e. when stereo-pairs are available for at least one date). The derived inventory and displacement fields of 169 slow-moving landslides show a positive relationship between the landslide size and velocities, as well as a seasonal acceleration of the largest landslides in response to an increase in effective precipitation. The processing technique can be adapted to better exploit increasingly available time-series from a variety of optical satellites for the detection and monitoring of landslide displacement [3].

The aim of this work is to present a spatio-temporal pixel-swapping algorithm (STPSA), based on conventional pixel swapping algorithms (PSAs), in which both spatial and temporal contextual information from previous land cover maps or observed samples are well integrated and utilized to improve sub pixel mapping accuracy. Unlike conventional pixel-swapping algorithms, STPSA is capable of utilizing prior information, which was previously ignored, to predict the attractiveness based on pairs of sub pixels. This algorithm involves three main steps and operates in an iterative manner: 1) it predicts the maximum and minimum attractiveness of each pair of pixels; 2) ranks the swapping scores based on the attractiveness of all the pairs; and 3) swaps the locations of the pair of pixels with a maximum score to increase the objective function. Experiments with actual satellite images have demonstrated that the proposed algorithm performs better than other algorithms. In comparison, the proposed STPSA's better performance is due to the fact that prior information used in other algorithms is restricted to a percentage level rather than the real sub pixel level [4].

Estimation of evapotranspiration (ET) from remote sensing based energy balance models have evolved as a promising tool in the field of water resources management. Performance of energy balance models and reliability of ET estimates is decided by the availability of remote sensing data at high spatial and temporal resolutions. The huge tradeoff in the spatial and temporal resolution of satellite images act as major constraints in deriving ET at fine spatial and temporal resolution using remote sensing based energy balance models. Hence a need exists to derive finer resolution data from the available coarse resolution imagery, which could be applied to deliver ET estimates at scales to the range of individual fields. The current study work employed a spatio-temporal disaggregation method to derive fine spatial resolution (60m) images of NDVI by integrating the information in terms of crop phenology derived from time series of MODIS NDVI composites with fine resolution NDVI derived from a single AWiFS data acquired during the season. The disaggregated images of NDVI at fine resolution were used to disaggregate MODIS LST data at 960 m resolution to the scale of Landsat LST data at 60 m resolution. The robustness of the algorithm was verified by comparison of the disaggregated NDVI and LST with concurrent NDVI and LST images derived from Landsat ETM+. The results showed that disaggregated NDVI and LST images compared well with the concurrent NDVI and LST derived from ETM+ at fine resolution with a high Nash Sutcliffe Efficiency and low Root Mean Square Error. The proposed disaggregation method proves promising in generating time series of ET at fine resolution for effective water management [5].

PROPOSED METHOD

The complete design flow involves the following steps like Input, Initialization, update

and output.

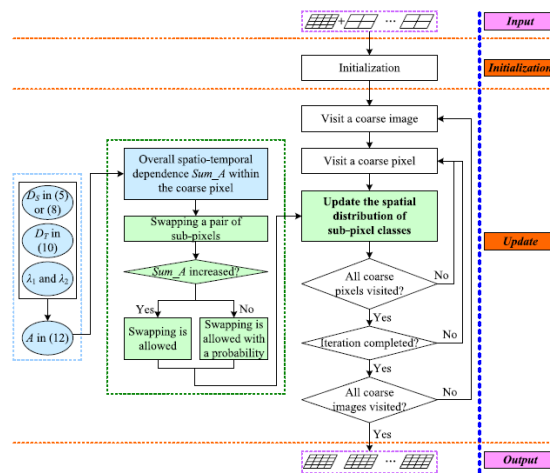


Figure 1: Flow diagram of the Spatiotemporal SPM algorithm

Step1: Input is a set of proportion image for all TSIs.

Step2: Initialization involves the allocation of sub pixels for each class in each image. For this process simple SPM techniques are used. In this work SPSAM is used for initialization. After initialization the subpixel location may vary but there won't be any variation in the number of sub pixel for each class of the image.

Step3: The update process is based on the cascade approach. Following are the steps involved in the update

1) SPM is conducted for each coarse image, in units of coarse pixels.

2) Let the current coarse image be \mathbf{I}_t , within a particular coarse pixel P_j^t , the following steps are implemented.

a) For all sub pixels, the sum of spatiotemporal dependence is calculated

The sum of spatial dependence for all S^2 subpixels is calculated by using $D_S^{SS}(i, j; t)$ in equation (1) or $D_S^{SP}(i, j; t)$ in equation (2).

$$D_S^{SS}(i, j; t) = \frac{1}{N_{SS}} \sum_{m=1}^{N_{SS}} \sum_{k=1}^K w_{SS}(p_{ij}^t, p_m^t) B_k(p_{ij}^t) B_k(p_m^t) \quad - (1)$$

$$D_S^{SP}(i, j; t) = \sum_{k=1}^K F_k(p_{ij}^t) B_k(p_{ij}^t) \quad - (2)$$

Then, with the temporal neighbors in images from the FSRM to \mathbf{I}_{t-1} (if the time of \mathbf{I}_t is after the FSRM) or \mathbf{I}_{t+1} (if the time of \mathbf{I}_t is before the FSRM), the sum of temporal dependence for all S^2 subpixels is calculated by using $D_T(i, j; t)$ in equation (3).

$$D_T(i, j; t) = \frac{1}{N_T} \sum_{r=1}^{N_T} \sum_{k=1}^K w_T(p_{ij}^t, p_{ij}^r) B_k(p_{ij}^t) B_k(p_{ij}^r) \quad - (3)$$

For all S^2 subpixels, the sum of spatiotemporal dependence is calculated according to equation (4).

$$A(i, j; t) = \lambda_1(t) D_S(i, j; t) + \lambda_2(t) D_T(i, j; t)$$

- (4)

b) A pair of sub pixels with different class labels is selected randomly, and their spatial locations are swapped. The sum of spatiotemporal dependence for all sub pixels in the new configuration is calculated again. If the overall spatiotemporal dependence increases, the swap is accepted; otherwise, the swap is allowed with a certain probability determined according to the current “temperature.” Such a probability decreases with the decreasing temperature at each iteration.

3) The steps a and b are repeated for each coarse pixel.

4) The swap process is repeated until the predefined number of iterations is reached for the current image I_t .

5) For each coarse image in the TSIs, steps 1–4 are implemented

ESTIMATION OF WEIGHT

The FSRM is used to obtain the weights of each pixel. Figure 2 shows the flowchart of the weight estimation method. In this example, the FSRM is assumed to be I_0 , and SPM goes from I_1 to I_t directly.

The detailed processes are described as follows.

Step 1: A weight pool is set for $\lambda l(x+n)$: $\{\lambda 1,1(x+n), \lambda 1,2(x+n), \dots, \lambda 1,L(x+n)\}$. In this paper, $\lambda 1(x+n)$ was varied from 0.1 to 0.9 with a step of 0.1, that is, the pool set is $\{0.1, 0.2, \dots, 0.9\}$.

Step 2: A weight $\lambda 1,l(x+n)$ ($l \in \{1, 2, \dots, L\}$) is selected from the pool, and the following procedures are conducted.

1) Regarding the FSRM as a starting point, spatiotemporal SPM of coarse images $I_{x+1}, I_{x+2}, \dots, I_{x+n}$ is performed with a zoom factor of S . In this process, the temporal information from the FSRM is propagated from I_{x+1} to I_{x+n} .

2) The FSRM is degraded with the factor of S to simulate the coarse images at that time.

3) SPM of the simulated coarse images for FSRM using the spatiotemporal model, in which the SPM results of $I_{x+1}, I_{x+2}, \dots, I_{x+n}$ are considered as temporally neighboring images.

4) The original FSRM is used for supervised assessment of the corresponding SPM result, and an accuracy value is recorded for the selected parameter.

Step 3: Step 2 is implemented for all weights in the pool, and L accuracy values are obtained as a result.

Step 4: The weight leading to the greatest accuracy is determined as the optimal one.

Step 5: Steps 1–4 are performed for the next coarse image I_{x+n+1} to estimate the corresponding weight $\lambda_1(x+n+1)$. The whole procedure is terminated after all coarse images are visited.

EXPERIMENTAL RESULTS:

The experiment was conducted on two different data sets to examine the proposed SPM algorithm. The data set images were captured at two different timing. Figures 3 and 4 represent the images captured at two different times respectively. The figure 5 shows the LCLU classified map. Figure 6 represent the synthesized images of the data set for three classes' water, urban and vegetation respectively. The figure 7 shows the block based analysis of both image1 and image2. Figure 8 shows the cell based analysis of the image1 and image2 which are captured at different time period.

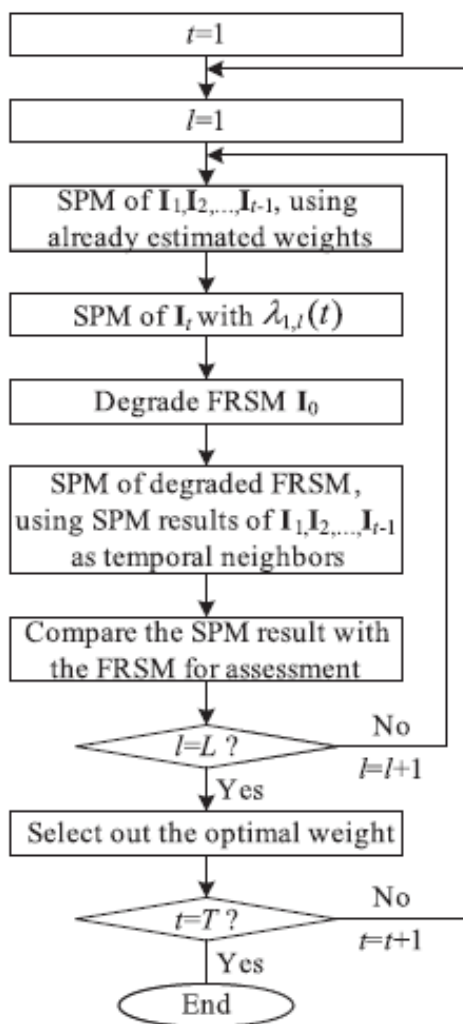


Figure 2: Flow chart of the weight estimation using the FRSM

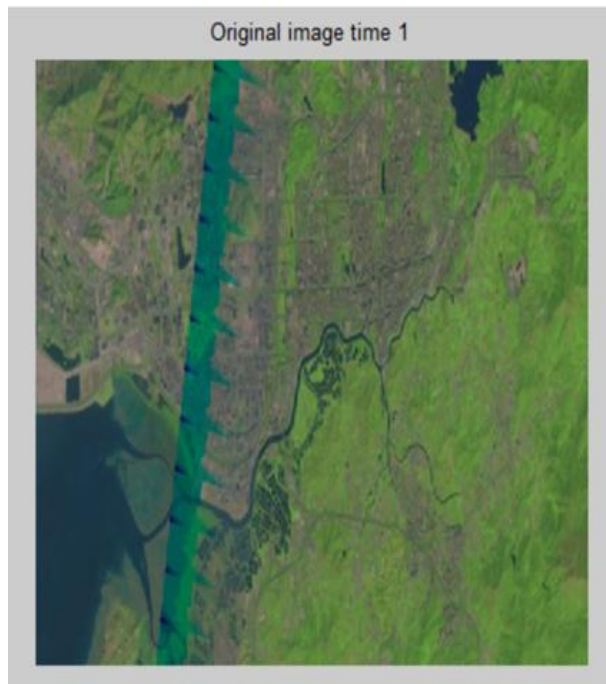


Figure 3: the images captured at time period 1

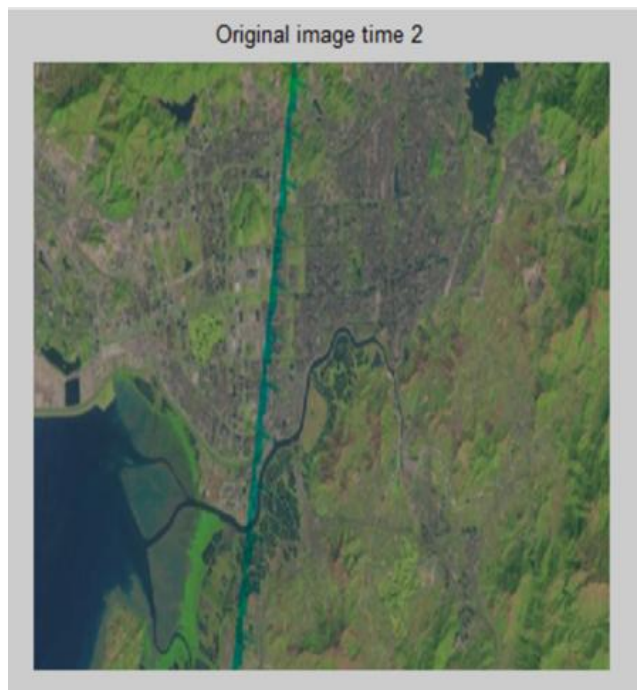


Figure 4: the images captured at time period 2

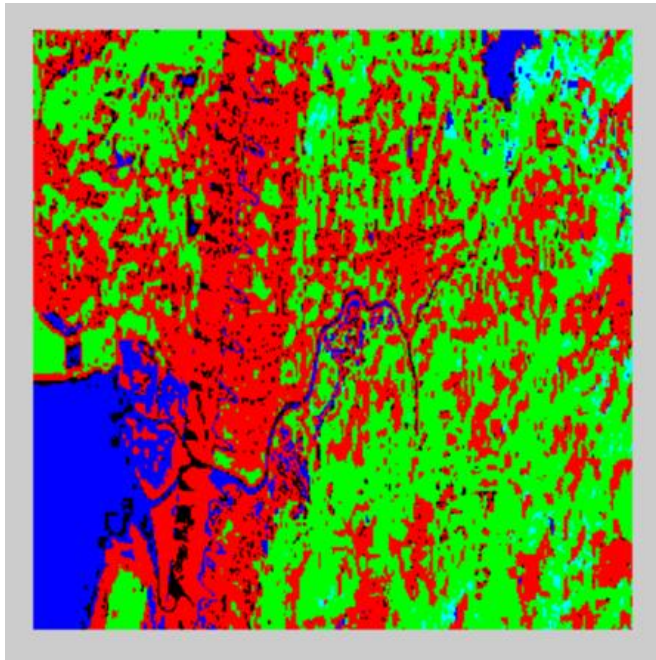


Figure5: The LCLU classified map of the image

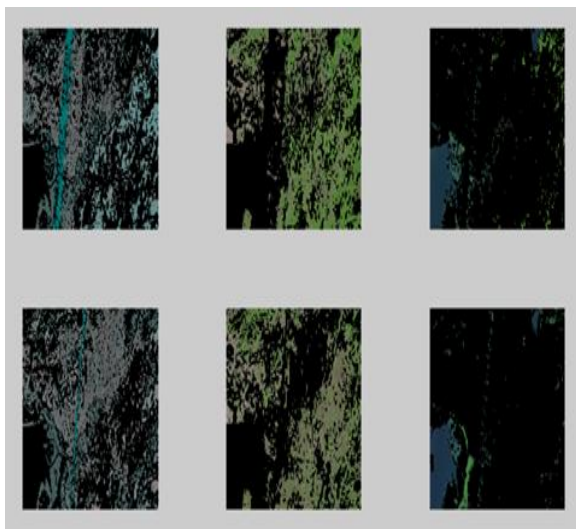


Figure 6: The synthesized images of the data set for three classes' water, urban and vegetation respectively

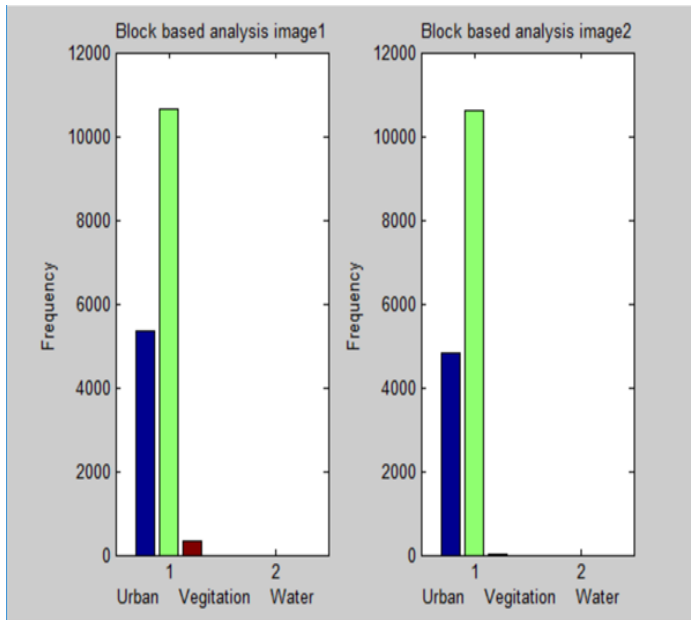


Figure 7: The block based analysis of both image1 and image2

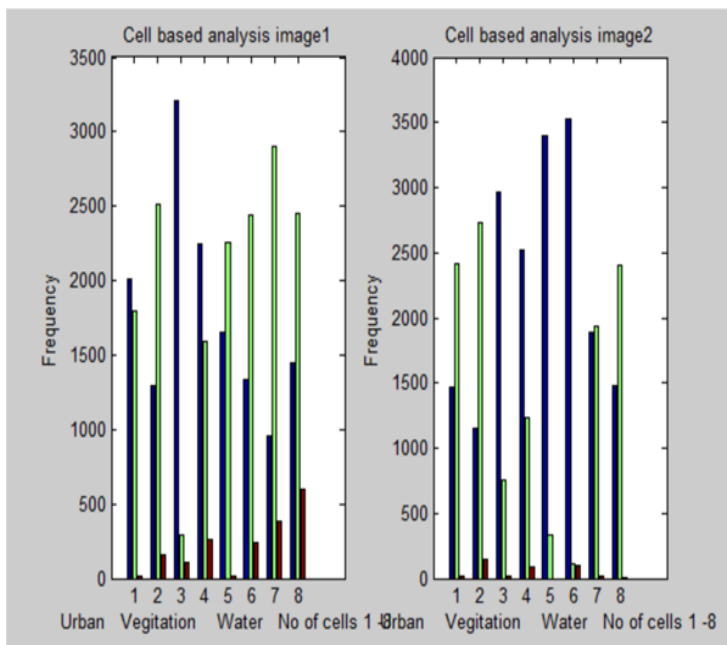


Figure 8: The Cell based analysis of both image1 and image2

CONCLUSION

The main objective of the proposed work is to increase the spatiotemporal dependencies in LCLU within each image and maximize the temporal dependencies in LCLU between images. The proposed SPM approach incorporates information from the FSRM in the TSIs. The various advantages of the proposed SPM approach are as follows: the spatial and temporal dependencies are considered simultaneously, readily incorporates multi resolution multi source data of TSIs, SPM is completely a automatic process and there is no human intervention in calculating the weights.

REFERENCES

- [1] P. H. Swain, "Bayesian classification in a time varying environment," *IEEE Trans. Syst., Man Cybern.*, vol. SMC-8, no. 12, pp. 879–883, Dec. 1978.
- [2] L. Bruzzone and S. B. Serpico, "An iterative technique for the detection of land-cover transitions in multitemporal remote-sensing images," *IEEE Trans. Geosci. Remote Sens.*, vol. 35, no. 4, pp. 858–867, Jul. 1997.
- [3] L. Bruzzone, D. F. Prieto, and S. B. Serpico, "A neural-statistical approach to multitemporal and multisource remote-sensing image classification," *IEEE Trans. Geosci. Remote Sens.*, vol. 37, no. 3, pp. 1350–1359, May 1999.
- [4] A. H. S. Solberg, T. Taxt, and A. K. Jain, "A Markov random field model for classification of multisource satellite imagery," *IEEE Trans. Geosci. Remote Sens.*, vol. 34, no. 1, pp. 110–113, Jan. 1996.
- [5] F. Melgani and S. B. Serpico, "A Markov random field approach to spatiotemporal contextual image classification," *IEEE Trans. Geosci. Remote Sens.*, vol. 41, no. 11, pp. 2478–2487, Nov. 2003.
- [6] D. Liu, M. Kelly, and P. Gong, "A spatial-temporal approach to monitoring forest disease spread using multi-temporal high spatial resolution imagery," *Remote Sens. Environ.*, vol. 101, no. 2, pp. 167–180, Mar. 2006.
- [7] K. Bahirat, F. Bovolo, L. Bruzzone, and S. Chaudhuri, "A novel domain adaptation Bayesian classifier for updating land-cover maps with class differences in source and target domains," *IEEE Trans. Geosci. Remote Sens.*, vol. 50, no. 7, pp. 2810–2826, Jul. 2012.
- [8] Y. Tarabalka, G. Charpiat, L. Bruker, and B. H. Menze, "Spatio-temporal video segmentation with shape growth or shrinkage constraint," *IEEE Trans. Image Process.*, vol. 23, no. 9, pp. 3829–3840, Sep. 2014.
- [8] [16] K. C. Mertens, L. P. C. Verbeke, E. I. Ducheyne, and R. De Wulf, "Using genetic algorithms in sub-pixel mapping," *Int. J. Remote Sens.*, vol. 24, no. 21, pp. 4241–4247, 2003.

- [9] Q. Wang, L. Wang, and D. Liu, "Particle swarm optimization-based subpixel mapping for remote-sensing imagery," *Int. J. Remote Sens.*, vol. 33, no. 20, pp. 6480–6496, 2012.
- [10] P. M. Atkinson, "Sub-pixel target mapping from soft-classified, remotely sensed imagery," *Photogramm. Eng. Remote Sens.*, vol. 71, no. 7, pp. 839–846, 2005.
- [11] A. Villa, J. Chanussot, J. A. Benediktsson, C. Jutten, and R. Dambreville, "Unsupervised methods for the classification of hyperspectral images with low spatial resolution," *Pattern Recognit.*, vol. 46, pp. 1556–1568, 2013.
- [12] A. J. Tatem, H. G. Lewis, P. M. Atkinson, and M. S. Nixon, "Superresolution land cover pattern prediction using a Hopfield neural network," *Remote Sens. Environ.*, vol. 79, pp. 1–14, 2002.
- [13] A. M. Muad and G. M. Foody, "Impact of land cover patch size on the accuracy of patch area representation in HNN-based super resolution mapping," *IEEE J. Sel. Topics Appl. Earth Observ. Remote Sens.*, vol. 5, no. 5, pp. 1418–1427, Oct. 2012.
- [14] Y. Zhong, Y. Wu, X. Xu, and L. Zhang, "An adaptive subpixel mapping method based on MAP model and class determination strategy for hyperspectral remote sensing imagery," *IEEE Trans. Geosci. Remote Sens.*, vol. 53, no. 3, pp. 1411–1426, Mar. 2015.
- [15] K. C. Mertens, B. D. Baset, L. P. C. Verbeke, and R. De Wulf, "A sub-pixel mapping algorithm based on sub-pixel/pixel spatial attraction models," *Int. J. Remote Sens.*, vol. 27, no. 15, pp. 3293–3310, 2006.
- [16] Z. Mahmood, M. A. Akhter, G. Thoonen, and P. Scheunders, "Contextual subpixel mapping of hyperspectral images making use of a high resolution color image," *IEEE J. Sel. Topics Appl. Earth Observ. Remote Sens.*, vol. 6, no. 2, pp. 779–791, Apr. 2013.
- [17] K. C. Mertens, L. P. C. Verbeke, T. Westra, and R. De Wulf, "Sub-pixel mapping and sub-pixel sharpening using neural network predicted wavelet coefficients," *Remote Sens. Environ.*, vol. 91, pp. 225–236, 2004.
- [18] Y. Shao and R. S. Lunetta, "Sub-pixel mapping of tree canopy, impervious surfaces, and cropland in the Laurentian great lakes basin using MODIS time-series data," *IEEE J. Sel. Topics Appl. Earth Observ. Remote Sens.*, vol. 4, no. 2, pp. 336–347, Jun. 2011.
- [19] J. Verhoeve and R. De Wulf, "Land-cover mapping at sub-pixel resolutions using linear optimization techniques," *Remote Sens. Environ.*, vol. 79, no. 1, pp. 96–104, 2002.
- [20] A. Boucher and P. C. Kyriakidis, "Super-resolution land cover mapping with indicator geostatistics," *Remote Sens. Environ.*, vol. 104, no. 3, pp. 264–282, 2006.
- [21] H. Jin, G. Mountrakis, and P. Li, "A super-resolution mapping method using local indicator variograms," *Int. J. Remote Sens.*, vol. 33, no. 24, pp. 7747–7773, 2012.

- [22] Q. Wang, P. M. Atkinson, and W. Shi, "Indicator cokriging-based subpixel mapping without prior spatial structure information," *IEEE Trans. Geosci. Remote Sens.*, vol. 53, no. 1, pp. 309–323, Jan. 2015.
- [23] T. Kasetkasem, M. K. Arora, and P. K. Varshney, "Super-resolution landcover mapping using a Markov random field based approach," *Remote Sens. Environ.*, vol. 96, no. 3/4, pp. 302–314, 2005.
- [24] V. A. Tolpekin and A. Stein, "Quantification of the effects of land-cover class spectral separability on the accuracy of Markov-random-field based superresolution mapping," *IEEE Trans. Geosci. Remote Sens.*, vol. 47, no. 9, pp. 3283–3297, Sep. 2009.
- [25] X. Li, F. Ling, Y. Du, and Y. Zhang, "Spatially adaptive superresolution land cover mapping with multispectral and panchromatic images," *IEEE Trans. Geosci. Remote Sens.*, vol. 52, no. 5, pp. 2810–2823, May 2014.
- [26] Y. F. Su, G. M. Foody, A. M. Muad, and K. S. Cheng, "Combining pixel swapping and contouring methods to enhance super-resolution mapping," *IEEE J. Sel. Topics Appl. Earth Observ. Remote Sens.*, vol. 5, no. 5, pp. 1428–1437, Oct. 2012.